Materials Science and Engineering B 178 (2013) 682–685

Contents lists available at SciVerse ScienceDirect

Materials Science and Engineering B

journal homepage: www.elsevier.com/locate/mseb

Short communication

Characterization of laser-induced damage in silicon solar cells during selective ablation processes

G. Poulain[a,b], D. Blanc[a,*], A. Focsa[a], M. De Vita[a], K. Fraser[a], Y. Sayad[c], M. Lemiti[a]

[a] Université de Lyon; Institut des Nanotechnologies de Lyon INL-UMR5270, CNRS, INSA de Lyon, Bâtiment Blaise pascal, Villeurbanne, F-69621, France
[b] Agence de l'environnement et de la Maîtrise de l'Energie, 20, avenue du Grésillé, BP 90406 49004 Angers Cedex 01, France
[c] Institut de Sciences et Technologies, Centre Universitaire de Souk Ahras, Route de Annaba, Souk Ahras, Algeria

ARTICLE INFO

Article history:
Received 26 June 2012
Received in revised form 7 November 2012
Accepted 25 November 2012
Available online 7 December 2012

Keywords:
Laser processing
Dielectric ablation
Minority carrier lifetime
Photoluminescence
Silicon solar cells

ABSTRACT

Selective laser ablation of silicon nitride layers on crystalline silicon wafers was investigated for solar cell fabrication. Laser processing was performed with a nanosecond UV laser at various energy densities ranging from 0.2 to 1.5 J cm^{-2}. Optical microscopy was used as a simple mean to assess the ablation threshold that was correlated to the temperature at the interface between the silicon nitride coating and the silicon substrate. Minority carrier lifetime measurements were performed using a microwave photoconductance decay technique. Band to band photoluminescence spectroscopy proved to be a sensitive technique to qualify the laser-induced damage to the silicon substrate. The crystalline structure of silicon seemed to be maintained after silicon nitride ablation as shown by UV reflectivity measurements. Laser parameters corresponding to fluences of around 0.4 J cm^{-2} were found to achieve selective ablation of SiN_x without causing detrimental damage to the surrounding material.

1. Introduction

Lasers are widely used for solar cell fabrication because of their potentially high throughput and spatial selectivity. Common laser uses include edge isolation, localised dopant diffusion and selective ablation of dielectrics. The latter finds application in wafer-based silicon solar cell manufacturing where ablation of the anti-reflection coating is necessary to selectively open areas before metallisation and in thin film manufacturing where several patterning steps are necessary to cut through the different layers. The challenge of laser ablation is to achieve complete removal of selected areas without causing damage to the surrounding material. More specifically, selective laser ablation of silicon nitride (SiN_x) has been studied recently for front and back contact metallisation technologies [1,2]. Comparisons between laser characteristics like wavelength and pulse duration have been performed to optimise the process windows [3,4]. In this work, laser ablation of SiN_x on p-type crystalline silicon wafers was investigated. The effect of the fluence or energy density from a nanosecond UV laser was studied using various techniques. Simulation was developed to describe the mechanism of laser ablation. The heat transfer equation was solved to relate the experimental observations to the temperature evolution at the interface between the silicon substrate and the SiN_x coating. Optical microscopy was used as a simple mean to assess the ablation threshold and the surface quality. Minority carrier lifetime was measured before and after ablation of SiN_x using the photoconductive decay technique. The crystalline structure of silicon was assessed by UV reflectivity measurements. Room temperature photoluminescence has been extensively used recently for silicon wafer and solar cell characterization [5–7]. In this work the decrease of the photoluminescence intensity associated with band to band recombination was directly related to the laser induced damage. Simulations were carried out to link the experimental data to surface recombination. Overall results were used to draw conclusions on the potential of laser processing for selective ablation of dielectrics in solar cell fabrication.

2. Selective ablation mechanism

In general, laser ablation of dielectric results from vaporization of the material due to heat. If the material to be ablated has a poor absorption coefficient at the laser wavelength, as it is the case for stoichiometric SiN_x in the UV range, ablation can still take place due to absorption in a highly absorbing substrate. Modelling of laser interaction with a SiN_x coating over a silicon substrate was done using the commercial software COMSOL Multiphysics. Laser–matter interaction of one laser pulse was studied. The differential equation describing the thermal effects is the heat-transfer equation:

$$\rho(T)C_p(T)\frac{\partial T}{\partial t} = \nabla\left[k_{th}(T)\nabla T\right] + Q \quad (1)$$

* Corresponding author. Tel.: +33 472 43 72 86; fax: +33 472 43 85 31.
E-mail address: daniele.blanc@insa-lyon.fr (D. Blanc).

0921-5107/$ – see front matter © 2012 Elsevier B.V. All rights reserved.
http://dx.doi.org/10.1016/j.mseb.2012.11.015

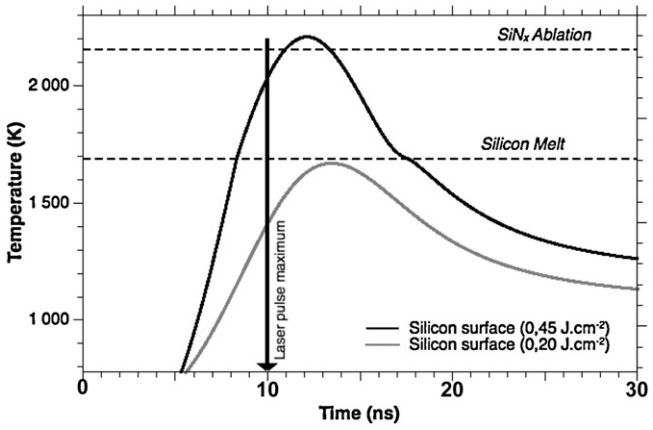

Fig. 1. Time evolution of the temperature at the Si/SiN_x interface for different laser fluences.

where $\rho(T)$ is the material density, $C_p(T)$ the specific heat capacity, T the temperature, t the time, k_{th} the thermal conductivity and Q the heat source per unit volume due to absorbed laser power. The heat source term can be written as follows:

$$Q = (1 - R(T))\alpha(T)P_{in}(x, t)I(y) \quad (2)$$

where $\alpha(T)$ is the material absorption coefficient, $R(T)$ the surface reflectivity, P_{in} the Gaussian incident laser power. $I(y)$ is the relative intensity given by the Beer–Lambert law and y the propagation direction of the laser beam:

$$I(y) = \exp\ (-\alpha(T)|y|) \quad (3)$$

Due to the low absorption coefficient of SiN_x at 355 nm ($\alpha_{SiN_x} \sim 3.5 \times 10^2 cm^{-1}$) compared to Si ($\alpha_{Si} \sim 10^6 cm^{-1}$) the laser absorption in SiN_x is negligible. Consequently the heat source term is around five orders of magnitude lower in SiN_x than in silicon. The heat absorbed in Si is transferred by conduction in a few nanoseconds to SiN_x. The Si substrate therefore behaves as a heat source after having absorbed the laser energy. The maximum temperature reached in SiN_x determines the ablation of the antireflection coating.

Fig. 1 shows the calculated temperature evolution at the Si surface for laser fluences of 0.2 and 0.45 J cm^{-2}. The shift in time between the maximum of the laser pulse of 10 ns duration at half maximum and the maximum temperature is related to the thermal diffusivity of Si. Melting of crystalline silicon takes place at 1680 K. For Si covered with SiN_x this temperature is reached at a laser fluence close to 0.2 J cm^{-2}. For comparison, melting of bare silicon in air is attained with a laser fluence of 0.6 J cm^{-2}. Decomposition of SiN_x occurs at a temperature around 2150 K. At this point the partial pressure of the N_2 in the SiN_x reaches one atmosphere which leads to the dielectric decomposition [3]. Simulation shows that SiN_x removal begins at an incident laser fluence about 0.4 J cm^{-2} in good agreement with the literature [4]. At lower laser fluence, below 0.4 J cm^{-2}, although SiN_x is not ablated, an area with a different optical appearance is observed indicating that the interface between silicon and SiN_x is thermally affected [8]. Indeed, melting of the silicon surface causes a deterioration of the Si/SiN_x interface due to the thermal expansion of the silicon in its liquid phase, corresponding to the observed thermally affected zone.

3. Sample preparation and characterization

3.1. Sample preparation

Double polished high quality p-type FZ crystalline silicon wafers were used for the characterization experiments. Wafers were 400 μm thick with a resistivity above 500 Ω.cm. SiN_x layers were deposited by PECVD on both surfaces. The properties of the layers were chosen to achieve a standard antireflection coating with a thickness of 75 nm and a refractive index around 2.01 at 635 nm. The laser used for ablation was a frequency tripled Nd:YAG laser with a Gaussian profile, a wavelength of 355 nm and a pulse duration of 10 ns and a repetition rate of 20 kHz. The beam diameter was around 25 μm. The system was equipped with a galvanometer head for fast beam scanning.

3.2. Optical microscopy

Typical optical microscope observations are shown in Fig. 2 for various laser energy densities ranging from 0.2 to 1.0 J cm^{-2}. As predicted by the calculation, the ablation threshold appeared around 0.4 J cm^{-2}. The percentage of ablated area was estimated to be around 20% for 0.2 J cm^{-2}, 80% for 0.4 J cm^{-2} and 100% above 0.6 J cm^{-2}. Partial removal below 0.4 J cm^{-2} is attributed to a poor pulse-to-pulse repeatability of the laser at low energy level, which causes significant variation of the fluence. No debris formation was noticeable below 0.8 J cm^{-2}. Severe damage with ablation of the silicon surface was observed from 1.0 J cm^{-2} upwards.

3.3. Photoconductance decay

Spatially resolved minority carrier lifetime mapping was performed before and after laser ablation by microwave photoconductance decay (Semilab WC-2000 μW-PCD), as shown in Fig. 3. Lifetime mapping of the passivated wafer (A) prior to ablation shows a reasonably homogeneous quality except on the edges. Small areas of 6 mm × 8 mm were ablated at different laser fluences. The remaining SiN_x was etched and both surfaces of the wafer passivated again with SiN_x before measurement (B). Dotted and plain squares correspond to laser fluences of 0.2 and 0.4 J cm^{-2} respectively. The sensitivity of the technique did not seem sufficient to distinguish clearly between the effects of the laser for fluences greater than 0.8 J cm^{-2}. Minority carrier lifetime dropped from around 550 μs on non-ablated areas to 100 μs after SiN_x ablation at 1.5 J cm^{-2} (Fig. 4). The ratio between these values should only be considered as an estimation of the laser induced damage because the starting wafer was not perfectly homogeneous. Considering the small penetration depth of the UV laser in

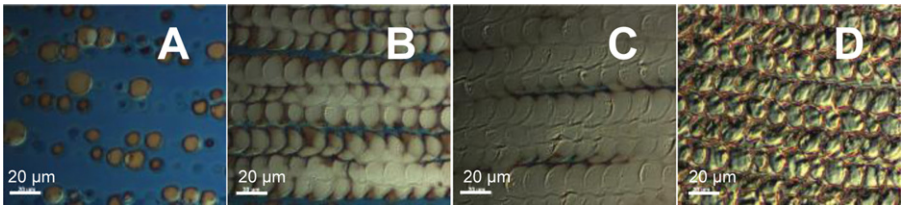

Fig. 2. Optical microscopy of ablated SiN_x on Si at fluences 0.2 J cm^{-2} (A), 0.4 J cm^{-2} (B), 0.6 J cm^{-2} (C), 1.0 J cm^{-2} (D). SiN_x appears in blue. (For interpretation of the references to color in this figure legend, the reader is referred to the web version of the article.)

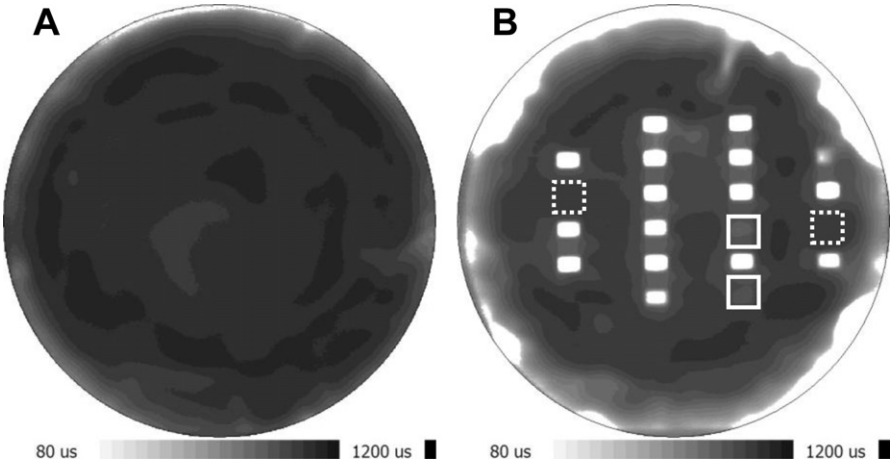

Fig. 3. Lifetime mapping of a passivated wafer before (A) and after (B) laser ablation at laser fluences between 0.2 and 1.5 J cm^{-2}. Dotted squares were ablated at 0.2 J cm^{-2} and plain squares at 0.4 J cm^{-2}.

silicon (around 10 nm), it was assumed that the decrease of the carrier lifetime was due to laser-induced defects located close to the surface.

3.4. Room temperature photoluminescence

Laser induced damage was further assessed by room temperature photoluminescence. At room temperature the emission spectrum of silicon consists of a broad band centered around 1134 nm related to the TO phonon-assisted band-to-band [9]. Room temperature PL spectra were recorded on passivated samples between 950 nm and 1300 nm with a spectral resolution of 2 nm. The excitation source was an 808 nm laser diode having a penetration depth in silicon of 13 μm, a spot size diameter of 1 mm and a power density of around 150 mW mm^{-2}. A set of spectra recorded on samples ablated at different laser fluences is shown in Fig. 5. The maximum photoluminescence intensity measured on a non-ablated sample was around 3 times larger than that measured after ablation at 0.2 J cm^{-2}. The insert shows spectra obtained at fluence 0.6 J cm^{-2} and above. Although the comparison of the photoluminescence intensity has to be considered carefully because of the non-homogeneity of the starting wafer, the technique appears very sensitive to laser-induced changes in silicon. We found that the photoluminescence intensity was reduced roughly by a factor of 10 when the laser fluence went from 0 (no ablation) to 0.4 J cm^{-2} while the PCD data decreased only by a factor of 2 for the same laser fluence variation. The difference in the overall response (factor 2 in the μ-PCD case, factor 10 in the photoluminescence case) could be explained by the lesser sensitivity of μ-PCD measurement to surface quality. The strong decrease of the maximum photoluminescence signal with increased laser fluence indicates the appearance of damage in Si.Simulations of photoluminescence were carried out to link the carrier recombination process to the laser-induced damage. The simulated photoluminescence signal was generated by using a finite difference model to compute the minority and majority carrier concentration under laser illumination as a function of depth. An increase in the concentration of defects near the surface as a result of laser ablation is represented as an increase in surface recombination velocity. The separation between data points in the simulation is 2.5 μm, much larger than the penetration depth of the UV laser, thus it is convenient to represent the ablation damage as surface states rather than bulk states. When the surface recombination velocity is varied in proportion to the change in fluence (for a suitable starting value at the lowest fluence), the normalized photoluminescence efficiency is found to follow the same trend as the experimental values, as shown in Fig. 6.

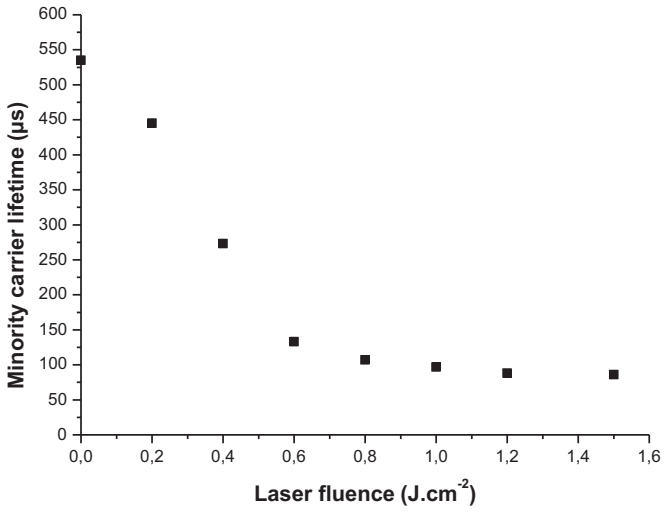

Fig. 4. Averaged minority carrier lifetime as a function of laser fluence measured by μW-PCD.

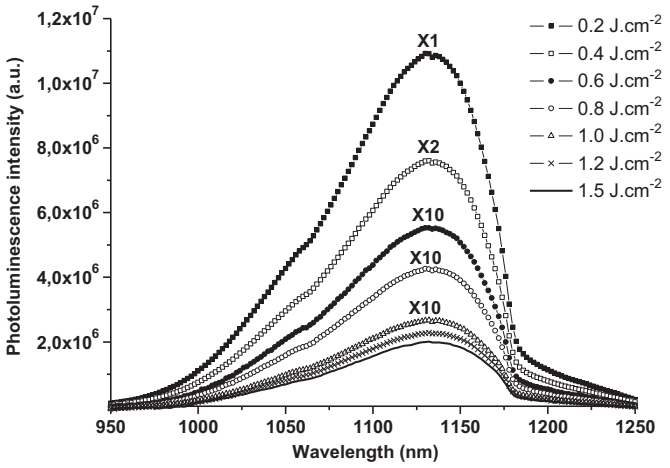

Fig. 5. Photoluminescence spectra of samples ablated with various laser fluences. The insert is an enlargement of the spectra for laser fluences above 0.6 J cm^{-2}.

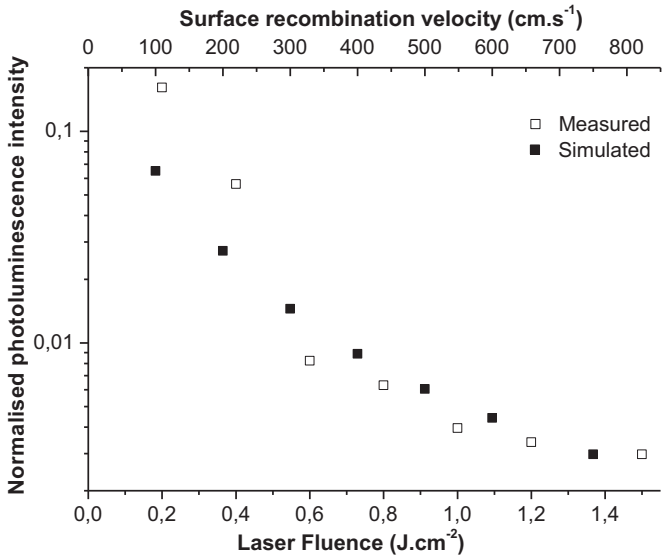

Fig. 6. Normalized variation of the photoluminescence intensity with laser fluence (full squares) and simulated photoluminescence intensity as a function of surface recombination velocity (hollow squares).

3.5. Reflectivity

The structure of silicon after laser ablation of SiN_x was investigated by reflectivity measurements as amorphisation of the surface would induce changes in the UV portion of the spectrum [10]. Total hemispherical reflectance measurements were made on bare silicon before and after laser ablation followed by a chemical etching of the surface in 2% HF. No obvious changes in the spectral shape were observed between the reference polished silicon and the samples ablated with different laser fluences as shown in Fig. 7. Two peaks are observed in the UV range around 290 nm and 365 nm even when high fluence was used for ablation. These peaks are attributed to direct optical transitions in crystalline silicon and are therefore a signature of the structure quality of the samples. The peak at 290 nm is normally expected around 270 nm. The shift is attributed to the response of the integrating sphere that shows a minimum around 270 nm.

Overall the characterization and modelling results show that the decrease of the average minority carrier lifetime and photoluminescence efficiency with laser fluence can be attributed to an increase of the surface recombination velocity linked to an increase in the concentration of defects near the surface. Reflectivity measurements suggest that these defects cannot be attributed to an amorphisation of the silicon surface as the crystalline structure of the surface seems to be preserved after the laser treatment. Further studies are needed to identify the nature of these defects (especially photoluminescence measurements at low temperature). Nevertheless, it is reasonable to assume that these defects are dislocations that appear at the interface between the melted zone and the bulk during cooling.

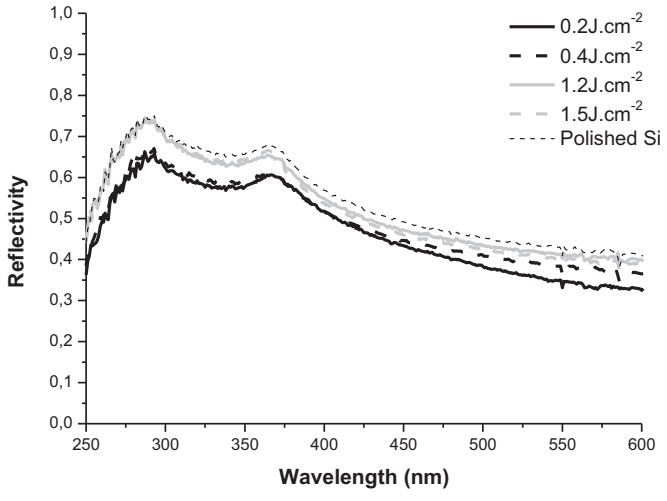

Fig. 7. Reflectivity spectra of bare silicon substrate after SiN_x ablation at different laser fluence.

4. Conclusion

Characterization using a variety of techniques shows the potential of UV laser processing for selective ablation of dielectrics. Laser ablation is found to locally remove SiN_x with minimum damage to the silicon substrate provided that the laser fluence stays in the range of $0.4\,J\,cm^{-2}$ or less. Simulations show that this fluence corresponds to the decomposition temperature of SiN_x. The large absorption coefficient of the UV light in silicon ensures a high energy deposition in a small volume and consequently an efficient ablation process. The pulse duration (10 ns) limits the thermal conduction to the surrounding material and allows for silicon re-crystallisation after melting. These observations confirm previous results obtained on industrial size solar cells where selective emitters were fabricated using laser ablation of SiN_x followed by a double diffusion process [11]. Furthermore, it was found that laser ablation of SiN_x led to slightly better electrical parameters than chemical etching when performed on laboratory scale solar cells with a 65 ohm/sq emitter. Although minority carrier lifetime is affected by the laser induced heating, silicon seems to retain its crystallographic order based on UV reflectivity spectra. Band-to-band room temperature photoluminescence appears as a sensitive technique to characterise laser–silicon interaction. Further studies are necessary to elucidate the nature of the induced defects.

Acknowledgements

This work was sponsored by the French Agency for Environment and Energy Management (ADEME) and by the French National Agency for Research through the project PROTERRA (ANR-10-HABISOL-010-02).

References

[1] A. Knorz, M. Peters, A. Grohe, C. Harmel, R. Preu, Progress in Photovoltaics: Research and Applications 17 (2009) 127–136.
[2] S. Hermann, T. Dezhdar, N.-P. Harder, R. Brendel, M. Seibt, S. Stroj, Journal of Applied Physics 108 (2010) 114514.
[3] S.A.G.D. Correia, J. Lossen, M. Wald, K. Neckermann, M. Bähr, Selective laser ablation of dielectric layers, in: Proceedings of 22nd European Photovoltaic Solar Energy Conference, Milan, Italy, 2007, pp. 1061–1067.
[4] V. Rana, Z. Zhang, C. Lazik, R. Mishra, T. Weidman, C. Eberspacher, Investigations into selective removal of silicon nitride using laser for crystalline silicon solar cells, in: Proceedings of 23rd European Photovoltaic Solar Energy Conference, Valencia, Spain, 2008, pp. 1942–1944.
[5] T. Trupke, J. Zhao, A. Wang, R. Corkish, M.A. Green, Applied Physics Letters 82 (2003) 2996–2998.
[6] T. Trupke, R.A. Bardos, M.C. Schubert, W. Warta, Applied Physics Letters 89 (2006) 044107–44113.
[7] J.A. Giesecke, M. Kasemann, W. Warta, Journal of Applied Physics 106 (2009) 014907–14908.
[8] G. Poulain, D. Blanc, A. Focsa, M. De Vita, B. Semmache, M. Gauthier, Y. Pellegrin, M. Lemiti, Energy Procedia 27 (2012) 516–521.
[9] M. Tajima, Journal of Crystal growth 103 (1990) 1–7.
[10] A. Straub, P.I. Widenborg, A. Sproul, Y. Huang, N. Harder, A.G. Aberle, Journal of Crystal Growth 265 (2004) 168–173.
[11] M. Gauthier, M. Grau, O. Nichiporuk, F. Madon, V. Mong-The Yen, N. Le Quang, A. Zerga, A. Slaoui, D. Blanc, A. Kaminski, M. Lemiti, Industrial approaches of selective emitter on multicrystalline silicon solar cells, in: 24th European Photovoltaic Solar Energy Conference, Hamburg, Germany, 2009, pp. 1875–1878.